

## INVESTIGATION ON THE EFFECTS OF STIFFNESS AND DAMPING COEFFICIENTS OF THE SUSPENSION SYSTEM OF A VEHICLE ON THE RIDE AND HANDLING PERFORMANCE

Mohammad ZEHSAZ<sup>1</sup>, Farid Vakili-TAHAMI<sup>2</sup>, Amin PAYKANI<sup>3</sup>

*Ride and handling characteristics of vehicles are the most important issues in the vehicle dynamic behavior. Therefore, this study examines the simultaneous behavior of ride comfort and good handling of vehicle by presenting a model with nine degrees of freedom. A computer code has been developed and used to solve this model with different parameters for the suspension system of a vehicle. The results show the effects of damping and stiffness of the system on three rotational motions, roll, pitch, and yaw. It has been shown that in cornering, by increasing the stiffness and damping, roll and pitch are reduced, but when passing through external bump, roll and pitch are increased.*

**Keywords:** Ride comfort and handling characteristics, vehicle dynamic behavior, suspension system

### 1. Introduction

One of the important factors in vehicle design is vehicle dynamic performance. Automotive manufacturers have tried to improve dynamic behavior of vehicles. When vehicle is moving, the vibration from the road surface negatively affects the ride comfort, handling stability and speed. Furthermore, this can also damage vehicle components. The purpose of vehicle's suspension system is to isolate the vehicle from the uncomfortable vibrations transmitted from the road through the tires and to transmit the control forces back to the tires so that the driver can keep the vehicle under control [1]. Numerous theoretical analyses and experimental studies have been carried out to propose methods resulting in better control of vehicle and getting the optimal performance of the suspension and steering systems for passengers' safety and comfort. For this purpose, different models have been developed which include simple linear model with one-degree-of-freedom and more complex and nonlinear models of rigid bodies. Simple vehicle models can provide an overall view of the vehicle behavior in certain conditions. But for a more detailed study, full vehicle model is used to study a wide range of different maneuvers and conditions. The simple linear models are valid only for systems with acceleration of less than 0.3g, so for the analysis of

<sup>1</sup> Universtiy of Tabriz, Islamic Republic Of Iran

<sup>2</sup> Universtiy of Tabriz, Islamic Republic Iran

<sup>3</sup> Universtiy of Tabriz, Islamic Republic Iran,e-mail: a.paykani@gmail.com

systems with higher accelerations, use of nonlinear models is essential [2]. Since the vehicle includes components such as suspension system, steering, brakes, transmissions and tires, the vehicle dynamic behavior depends on the behavior of all its components and to simulate the vehicle dynamic, acceptable dynamic models of each of these components must be obtained and used. Analytical or numerical simulations based on tires' geometric and physical properties, and their quality have been started since 1940 [3]. Usually, two types of models have been used to model the tire: in one type the tire is considered as a string and in the other type as a beam. In both of the models, the objective is to investigate the tire behavior in the range of its contact with the road surface area and the equations obtained based on it, give the forces and torques resulted from tire contact with the road bed. Although these models are complex, their results are relatively satisfactory. The history and complete discussion of the tire modeling can be found in Refs. [4-7].

One of the most simple and useful models for vehicle dynamic was presented by Segel which was the main base for the next theoretical and experimental researches [8]. In this model, three degrees of freedom rolling, rotation and lateral movement were considered for the vehicle. Since this model was linear, it was able to obtain rotational rate response, lateral acceleration and rolling speed towards the front wheel steering angle by using conversion functions in frequency domain.

In mid-1960, automobile companies in USA, Europe and Japan have began extensive researches in the field of steering ability, easy traveling, safety and vehicle design and its components using nonlinear modeling [9-10]. Examples of these models are the seven-degree-of-freedom model used by Toyota [11] and sustainability model developed in Chrysler [12]. Zhu et al. [13] used a seven-degrees-of-freedom model for the vehicle, this model was used to study the random vibrations of a nonlinear suspension system. In another study by Cation et al. [14] a-six-degrees-of-freedom model was used to study the applied vibrations into the chassis. In this system, non-suspended masses, including four wheels have been introduced which have independent movement or one degree of freedom. Also, cabin is included with two degrees of freedom which one of them is in the vertical direction and the other in angular movement around the longitudinal axis.

This study investigates the effect of stiffness and damping coefficients of the suspension system of a vehicle on the combined riding and handling performance of a vehicle by providing a model with nine-degrees-of-freedom, and discusses the results of the effects of vehicle damping and stiffness on three rotational motions: roll, pitch and yaw. In addition, stiffness and damping effect on turning radius of vehicles has been studied. The Lagrange method was used for writing equations of motion. Derived differential equations were solved using

SIMULINK. Also, a computer code has been developed using programming language DELPHI 6.0 to solve the governing differential equations. The results obtained using these two programs was compared to validate the solution method and its accuracy.

## 2. Vehicle dynamic simulation

In this study, a nonlinear model has been used in which the chassis is considered with five-degrees-of-freedom and wheels with four-degrees-of-freedom, so overall degrees of freedom for the vehicle-model is nine. Also, the front suspension system of the vehicle is assumed to be independent. Each of the front wheels has one degree of freedom in the vertical direction. The degrees of freedom for the right and left front wheels are shown by  $z_1$  and  $z_2$  respectively. The rear suspension system is considered as integrated with rigid axle and two degrees of freedom, one in the vertical direction  $z_3$  and the other rotational  $\gamma$ . The longitudinal vehicle dynamics is ignored and it is assumed that the vehicle moves in longitudinal direction with constant speed. Eq. (1) shows the governing equations of motion of the vehicle based on the Lagrange equations in terms of general coordinates.

$$\frac{d}{dt} \left( \frac{\partial T}{\partial \dot{q}_i} \right) - \frac{\partial T}{\partial q_i} + \frac{\partial V}{\partial q_i} + \frac{\partial D}{\partial \dot{q}_i} = Q_i \quad (1)$$

In this paper, inputs applied to the wheels through the road, are shown by  $u_1(t)$ ,  $u_2(t)$ ,  $u_3(t)$  and  $u_4(t)$  and applied input from the steering wheel of the vehicle to the wheels is shown by  $\delta(t)$ . It should be noted that, wheels not only have movement in vertical direction and yaw but also they move along with the body in x and y directions. Eq. (2) shows the total kinetic energy of the vehicle,

$$\begin{aligned} T = & \frac{1}{2} M (\dot{x}^2 + \dot{y}^2) + \frac{1}{2} M_s \dot{z} + \frac{1}{2} m_1 \dot{z}_1 + \frac{1}{2} m_2 \dot{z}_2 + \frac{1}{2} m_3 \dot{z}_3 + \\ & \frac{1}{2} I'_z \dot{\alpha}^2 + \frac{1}{2} I'_z \dot{\gamma}^2 + m' \dot{\alpha} \dot{\gamma} + \frac{1}{2} I_x (\dot{\phi} \cos \psi \cos \alpha + \dot{\psi} \sin \alpha)^2 + \\ & \frac{1}{2} I_y (\dot{\psi} \cos \alpha - \dot{\phi} \cos \alpha \sin \alpha)^2 + \frac{1}{2} I_z (\dot{\phi} \psi + \dot{\alpha})^2 \end{aligned} \quad (2)$$

In this equation, it has been assumed that  $m_1 = m_2 = \frac{M_{uf}}{2}$  and  $m_3 = M_{ur}$ .

where  $M_{uf}$  is the front unsprung mass and  $M_{ur}$  is rear unsprung mass.

$$I'_z = \frac{1}{2} \left[ m_1 \left[ l_f^2 + \frac{l_f^2}{4} \right] + m_2 \left[ l_f^2 + \frac{t_f^2}{4} \right] + m_3 I_r^2 \right] \quad (3)$$

where  $l_f$  is the longitudinal distances measured from the CG to the front axle. Suspension system consists of two basic energy- storing and dissipating elements, and their combined performance causes vehicle's smooth motion. In this paper, the suspension system is considered as a vibrating model including mass and damper. Linear spring and dampers are used to model the suspension system and the tire is modeled with two spring and damper which are connected to each other paralleled. Fig. 1 shows the degrees of freedom and establishment of the suspension system and front wheels. Eq. (4) gives the potential energy of the right-hand side spring obtained with regard to the displacement of its two ends.

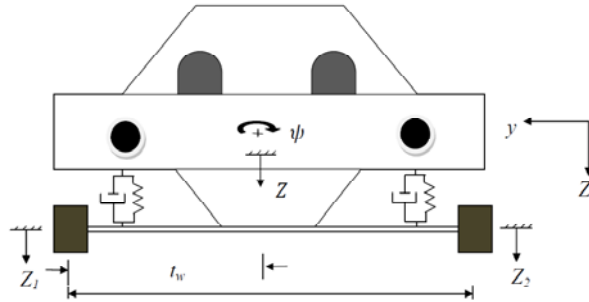


Fig. 1. degrees of freedom and establishment of the suspension system and front tires.

$$V_1 = \frac{1}{2} k_1 (\Delta z_1)^2 = \frac{1}{2} k_1 (z - l_f \psi + a \psi - \frac{t_s}{t_w} z_1)^2 \quad (4)$$

In this equation displacement equals:

$$\Delta z = z - l_f \psi + a \psi \quad (5)$$

where  $a$  is the transverse distance between the suspension springs and chassis's center of gravity that equals:

$$a = \frac{t_f}{2} - t_w + t_s \quad (6)$$

The relative displacements of two ends of right-hand side springs are obtained through Eq. (7),

$$z_1 = z - l_f \psi + a \psi - \frac{t_s}{t_w} z_1 \quad (7)$$

The potential energy of the left-hand side front spring is obtained using Eq. (8).

$$V_2 = \frac{1}{2}k_2(\Delta z_2)^2 = \frac{1}{2}k_2(z - l_f\psi + a\psi + a\varphi - \frac{t_s}{t_w}z_2)^2 \quad (8)$$

The front suspension has a balancing shaft (anti-twist), which controls the wheels, and its potential energy is obtained using Eq. (9),

$$V_5 = \frac{1}{2}k_{tf}\theta^2 = \frac{1}{2}k_{tf}\left(\frac{z_1 - z_2 - l''\varphi}{l'}\right)^2 \quad (9)$$

Fig. 2 shows the degrees of freedom and establishment of the front tires and suspension system. Eqs. (10) and (11) indicate the rear right spring and the rear left spring potential energies, respectively.

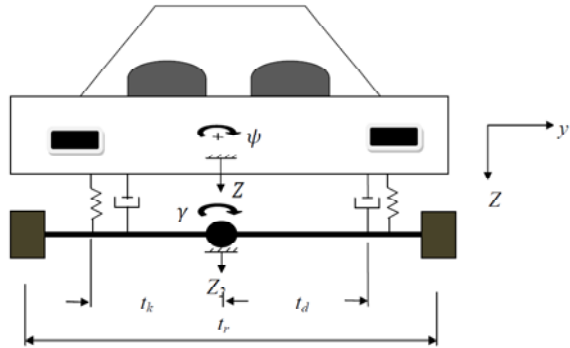


Fig. 2. degrees of freedom and establishment of the suspension system and rear tires.

$$V_3 = \frac{1}{2}k_r(\Delta z_3)^2 = \frac{1}{2}k_r(z + l_r\psi + t_k\varphi - z_3 - t_k\gamma)^2 \quad (10)$$

$$V_4 = \frac{1}{2}k_r(\Delta z_4)^2 = \frac{1}{2}k_r(z + l_r\psi - t_k\varphi - z_3 + t_k\gamma)^2 \quad (11)$$

If the tire stiffness value is equal to  $k_t$ , and the input  $u$  is applied to the tire from the road, potential energy of the front and rear tires is obtained from Eqs. (12) and (13),

$$V_6 = \frac{1}{2}k_t(z_1 - u_1)^2 + \frac{1}{2}k_t(z_2 - u_2)^2 \quad (12)$$

$$V_7 = \frac{1}{2}k_t(z_3 + \frac{t_r}{2}\gamma - u_3)^2 + \frac{1}{2}k_t(z_4 + \frac{t_r}{2}\gamma - u_4)^2 \quad (13)$$

Eq. (14) shows the overall potential energy of the vehicle,

$$V = V_g + V_1 + V_2 + V_3 + V_4 + V_5 + V_6 + V_7 \quad (14)$$

In which  $V_g$  is equal to:

$$V_g = M_g z + m_1 g z_1 + m_2 g z_2 + m_3 g z_3 + m_4 g z_4 \quad (15)$$

where  $M_g$  is the chassis mass and  $m_1, m_2, m_3$  and  $m_4$  are the wheels masses.

The suspension system has dampers which help to reduce the amplitude of the vibration of the vehicle by dissipating energy which can be calculated. In this

paper linear dampers are used and according to Rayleigh function, the term  $\frac{1}{2}C\dot{\Delta}^2$  is used to calculate the dissipated energy. In this term C is the spring damping coefficient and  $\dot{\Delta}$  is the relative speed of the two heads of the damper. Also, to model the energy dissipating effect of springs, a damper element has been added next to each spring. Differentiating the above equations gives the relative speed of damper ends. Also, using Lagrange equation (Eq. 1) the governing dynamic equations for the vehicle motion are achieved. In these equations  $q_i$  are the general coordinates or degrees of freedom which include variables, z,  $z_1$ ,  $z_2$ ,  $z_3$ ,  $\gamma$ ,  $\phi$ ,  $\Psi$  and  $\alpha$ .

The external forces on the vehicle are due to the tire contact with the ground or the aerodynamic forces and air resistance. Since, the longitudinal vehicle dynamics has not been considered in this research and the vehicle is moving in longitudinal direction at a constant speed, it would be possible to drop the effects of aerodynamic forces, braking forces, applied longitudinal forces from the driving wheels and longitudinal Rolling resistance. Fig. 3 depicts the general applied forces to the vehicle. Eqs. (16) to (19) show the components of the forces and torques applied to the vehicle. The forces along other degrees of freedom or either zero or they are given in terms of other dynamic equations.

$$\begin{aligned}
 D = & \frac{1}{2}c_f(\dot{z} - l_f\dot{\psi} + a\dot{\phi} - \frac{t_s}{t_w}\dot{z}_1)^2 + \frac{1}{2}c_f(\dot{z} - l_f\dot{\psi} - a\dot{\phi} \\
 & - \frac{t_s}{t_w}\dot{z}_2)^2 + \frac{1}{2}c_r \cos^2(\omega)(\dot{z} + l_r\dot{\psi} + t_d\dot{\phi} - z_3 - t_d\dot{\gamma})^2 + \\
 & \frac{1}{2}c_r \cos^2(\omega)(\dot{z} + l_r\dot{\psi} - t_d\dot{\phi} - z_3 + t_d\dot{\gamma})^2 + \frac{1}{2}c_t(\dot{z}_1 - \dot{u}_1)^2 \\
 & + \frac{1}{2}c_t(\dot{z}_2 - \dot{u}_2)^2 + \frac{1}{2}c_t(\dot{z}_3 + \frac{t_r}{2}\dot{\gamma} - \dot{u}_3)^2 + \frac{1}{2}c_t(\dot{z}_3 - \frac{t_r}{2}\dot{\gamma} - \dot{u}_4)
 \end{aligned} \tag{16}$$

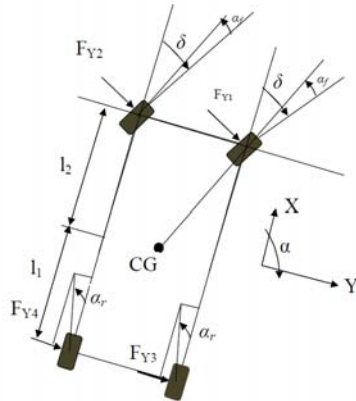


Fig. 3. Applied general forces on the vehicle.

$$Q = Q_x \delta_x + Q_y \delta_y + Q_\alpha \delta_\alpha \quad (17)$$

$$Q = (F_{y1} + F_{y2}) \cos \delta + (F_{y3} + F_{y4}) \quad (18)$$

$$Q_\alpha = (F_{y1} + F_{y2}) l_f \cos \delta - (F_{y3} + F_{y4}) l_r + 0.5 (F_{y1} - F_{y2}) t_f \sin \delta - M_{z1} - M_{z2} - M_{z3} - M_{z4} \quad (19)$$

The External forces are always applied to the tires due to the moving of the vehicle along the road, for example, when a maneuver is carried out in the vehicle, it causes lateral acceleration which consequently causes lateral force in the tire. By changing the vertical reaction force due to the change in the lateral acceleration, the applied forces on the wheels will also change. Therefore, developing a model that is able to implement this dependence would be inevitable. Different non-linear models have been proposed to simulate the forces between the tire and the road surface among those Kaspian's model was used in this research [14-16].

$$C_i = A_0 + A_1 F_{zi} - \frac{A_1}{A_2} \dot{F}_{zi} \quad (20)$$

In the above equation,  $A_0$ ,  $A_1$ ,  $A_2$  are Kaspian's coefficients which depend on the type of tire and  $F_{zi}$  is the vertical force applied on each wheel. Eq. (21) shows the lateral forces of the tires as a function of the vertical forces, slip angle, coefficient of the lateral stiffness, lateral friction coefficient, the maximum permissible load, tire camber angle, hardness due to tire camber angle and type of tire slip.

$$(F_{yi}) = SN \cdot \mu_{yi} \cdot F_{zi} \cdot f(\bar{\alpha}_l) + F_i \cdot \gamma_i \quad (21)$$

In this equation  $f(\alpha_l)$  is the dimensionless function of the slip angle and is defined as Eq. (22).

$$f(\bar{\alpha}_l) = \bar{\alpha}_l - \frac{1}{3} \bar{\alpha}_l |\bar{\alpha}_l| + \frac{1}{27} \bar{\alpha}_l^3 \quad (22)$$

And  $\alpha_i$  is the slip angle variable and is defined as follows:

$$\bar{\alpha}_l = \frac{c_i \alpha_i}{(s_i)_{\max}} \quad (23)$$

The governing differential equations of motion with nine-degrees-of-freedom derived using equations of state, reduced from second order to the first order and then are solved using SIMULINK program from MATLAB software. In this approach, the second order differential equations were converted to first order differential equations using state equations. Then, state equations were substituted within the following equation

$$\begin{aligned}
& (I_x \cos^2 \alpha + I_y \sin^2 \alpha + I_z \psi^2 + 2(I_{xz} \cos \alpha - I_{yz} \sin \alpha) \psi) \ddot{\varphi} + \\
& (I_x \frac{\sin 2\alpha}{2} - I_y \frac{\sin 2\alpha}{2} + (I_{xz} \sin \alpha + I_{yz} \cos \alpha) \psi) \ddot{\psi} + \\
& (I_z \psi + (I_{xz} \cos \alpha - I_{yz} \sin \alpha)) \ddot{\alpha} = F_\varphi
\end{aligned} \tag{24}$$

$$\begin{aligned}
& m \ddot{y} + (I_z \psi + I_{xz} \cos \alpha - I_{yz} \sin \alpha) \ddot{\varphi} + (I_{yz} \cos \alpha \\
& + I_{xz} \sin \alpha) \ddot{\psi} + (I_z + I'_z) \ddot{\alpha} = F_\alpha \\
& (I_x \frac{\sin 2\alpha}{2} - I_y \frac{\sin 2\alpha}{2} + (I_{xz} \sin \alpha + I_{yz} \cos \alpha) \psi) \ddot{\varphi} \\
& + I_x (I_x \sin^2 \alpha + I_y \cos^2 \alpha) \ddot{\psi} + \\
& (I_{xz} \sin \alpha + I_{yz} \cos \alpha) \ddot{\alpha} = F_\psi \\
& (I_{xz} \sin \alpha + I_{yz} \cos \alpha) \ddot{\alpha} = F_\psi
\end{aligned} \tag{25}$$

Then, all of equations are obtained in the below form.

$$\dot{X}_i = F(X_1, X_2, X_3, \dots, X_{18}, t) \tag{26}$$

### 3. The road inputs

For dynamic analysis of the vehicle and its suspension system the following inputs have been considered.

#### 3.1. Smooth road inputs

In this case vehicle passes through the smooth surface. The effects of road surface were not applied in this analysis.

$$u_1(t) = u_2(t) = u_3(t) = u_4(t) = 0 \tag{27}$$

This case was considered in order to observe the direct effect of the vehicle steering and acceleration on the response.

#### 3.2. Random input

Another type of input which models the road surface profile is the random vibrations which are the combination of a number of sinusoidal random waves. This type of input data describes the type of common roads and pavements.

$$f(t) = \sum_{i=1}^M A(f) \sin[2\pi f i t + \theta(f)] \tag{28}$$

In this equation  $A(f)$  is the amplitude of the road roughness spectrum,  $f$  is the frequency of road roughness,  $t$  is time,  $M$  is the number of harmonics,  $\theta(f)$  is the phase angle ( $\theta(f) = 2\pi(RND - 0.5)$ ,  $0 < RND < 1$ ). Where RND is a random number [17].

### 3.3. Bump input

This model shows the possible bumps that vehicles may face in some cases. In this type of model two wheels of the one side of the vehicle are passing through a bump in a specific time interval. With this type of input, it would be possible to examine the performance or effect of stiffness, the dampers, and front and rear suspension mechanisms and also the roll, pitch and vertical movement of the body. In this case, the wheels of one side of the vehicle or all wheels or just one of the wheels enter into the bump. This type of input can be in the form of depressions or bumps. If the distance between the two axles of the vehicle is  $L$  and vehicle is in motion with speed of  $V$ , the rear wheels will enter the bump with the delay time of  $T = L / V$ . Therefore, the input is defined as  $u(t) = U(t-T)$  for the rear wheels. Eq. (29) shows the profile of the bump.

$$U(t) = \begin{cases} \frac{-t}{2} & 0 \leq t \leq 0.1 \\ -0.05 & 0.1 \leq t \leq 0.4 \\ \frac{(t-0.5)}{2} & 0.4 \leq t \leq 0.5 \\ 0 & t \geq 0.5 \end{cases} \quad (29)$$

## 4. Steering input and Driver's maneuvers

This case is used to study and analyze the performance of the suspension and steering systems and also the effects of the different inputs of the steering on the dynamic behavior of the vehicle.

### 4.1. Vehicle moving along the horizon without applying steering

In this case, there is no steering input, and the aim is to evaluate the effects of the road input or effects of the acceleration and braking. Movements involving with ride appear in this type of input.

### 4.2. The motion to change the line

In this case, the change of moving direction is modeled. This type of input is used to study the handling.

### 4.3. Step steer

This type of input, like Lane change, is used for the good handling. Under steering or over steering situations can be realized using this model.

Table 1 shows the dimensions, sizes and parameters which are used to perform the simulation.

Table 1

The parameters used for the simulation [18-19-20].

$c_f$	$c_r$	$C_t$	$g$	$h_{cg}$	$h_f$	$h_r$	$I_x$
2000 (N.sec/m)	1500 (N.sec/m)	200 (N.sec/m)	9.81 (m/s <sup>2</sup> )	500 (mm)	270 (mm)	270 (mm)	500 (kg.m <sup>2</sup> )
$I_y$	$I_z$	$I_{xy}$	$I_{yz}$	$I_{xz}$	$I'_x$	$k_f$	$k_r$
2460 (kg.m <sup>2</sup> )	3200 (kg.m <sup>2</sup> )	0	100 (kg.m <sup>2</sup> )	150 (kg.m <sup>2</sup> )	70 (kg.m <sup>2</sup> )	20000 (N/m)	20000 (N/m)
$k_t$	$k_{tf}$	$l_f$	$l_r$	$l'$	$l''$	$M_s$	$m_l$
175500 (kN/m)	2000 (kN.Rad/m)	1300 (mm)	1500 (mm)	800 (mm)	200 (mm)	850 (kg)	40 (kg)
$m_2$	$m_3$	$t_f$	$t_r$	$t_d$	$t_k$	$t_s$	$t_w$
40 (kg)	71 (kg)	1522 (mm)	1501 (mm)	600 (mm)	700 (mm)	500 (mm)	600 (mm)
$\gamma$	$\omega$						
1°	2°						

## 5. Results and discussion

In this study the effects of vehicle stiffness and damping on the rotational motions roll, pitch and yaw are investigated. It should be noted that various inputs have different effects on these motions. In the first analysis, a step steer is applied in accordance with Fig. 4 and the effects of changes in the vehicle stiffness and damping on three rotational motions roll, pitch and yaw are investigated. The vehicle speed was set to be 108 km/h. In the second analysis the steering input is trajectory (Lane change). The vehicle speed was considered as 90 km/h. The maximum roll of the chassis for step-steer and Lane change, based on changes in the front and rear stiffness is shown in Fig. 5. As it can be seen, by increasing the rigidity of front and rear wheels, the amount of roll reduces. Fig. 6 shows the displacement of the chassis with changing the front and rear stiffness in a given time period which indicates an increase in the value of yaw with increasing the stiffness of the suspension system. Increasing the stiffness of the system results in reduction of the pitch value. But as it can be seen in Fig. 7, because the pitch is a good riding parameter and usually it is less excited in steering input motions, therefore, sometimes it is ignored in good handling analysis.

Figs. 8 to 10 demonstrate the variations of roll, pitch and yaw parameters with variation of vehicle damping obtained for the case with steering input as a step. These figures show the similar pattern for the change of damping coefficient with those obtained for the change of stiffness.

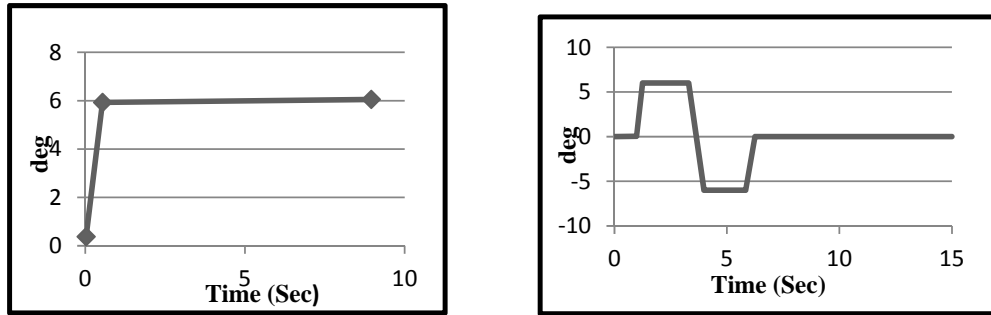


Fig. 4 Step steer input and Lane change input

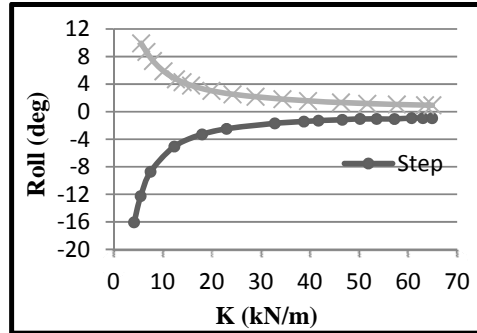


Fig. 5 Maximum chassis Roll based on changes in the vehicle front and rear stiffness for the step steer and Lane change.

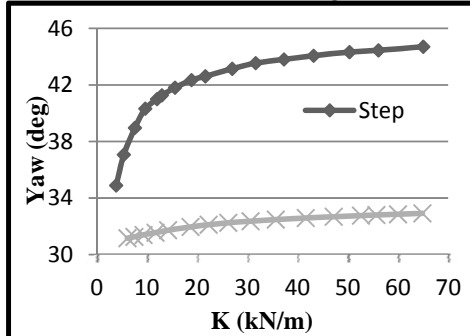


Fig. 6 The vehicle chassis deflection based on changes in the vehicle front and rear stiffness in a specific time period for the step steer and Lane change.

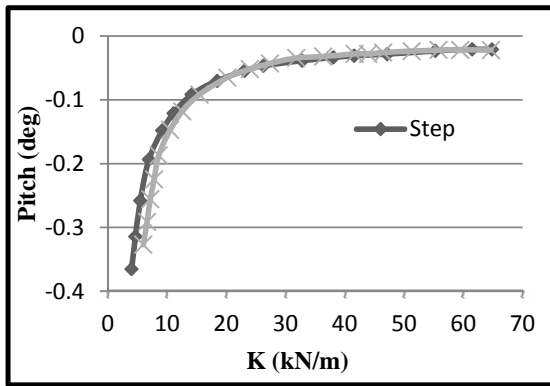


Fig. 7 Maximum chassis Pitch based on changes in the vehicle front and rear stiffness for the step steer and Lane change.

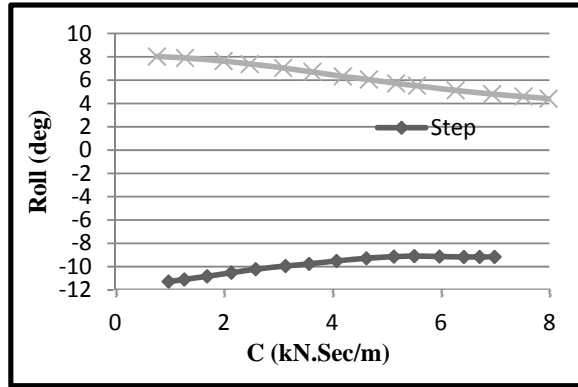


Fig. 8 Maximum chassis Roll based on changes in the vehicle front and rear damping for the step steer and Lane change.

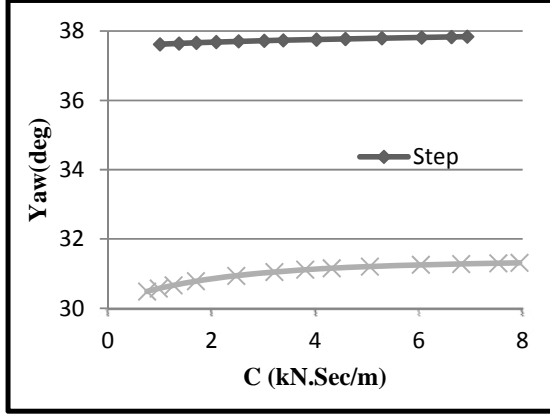


Fig. 9 The vehicle chassis deflection based on changes in the vehicle front and rear damping in a specific time period for the step steer and Lane change.

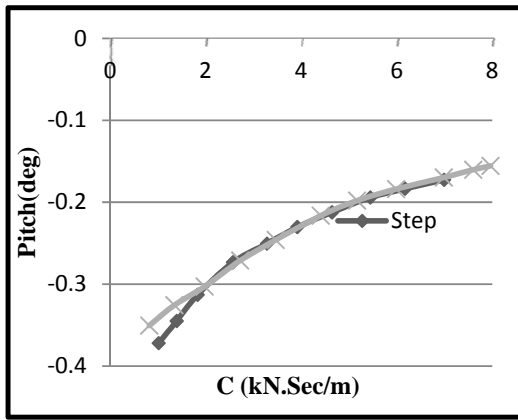


Fig. 10 Maximum chassis Pitch based on changes in the vehicle front and rear damping for the step steer and Lane change.

Fig. 11 depicts the maximum amount of vehicle lateral acceleration which is increased with increasing the stiffness but the vertical acceleration of the body decreases with increasing the stiffness. Also Fig. 12 shows the maximum amount of vehicle lateral speed for step wise steering and Lane change and it can be seen that it is reduces with increasing the stiffness.

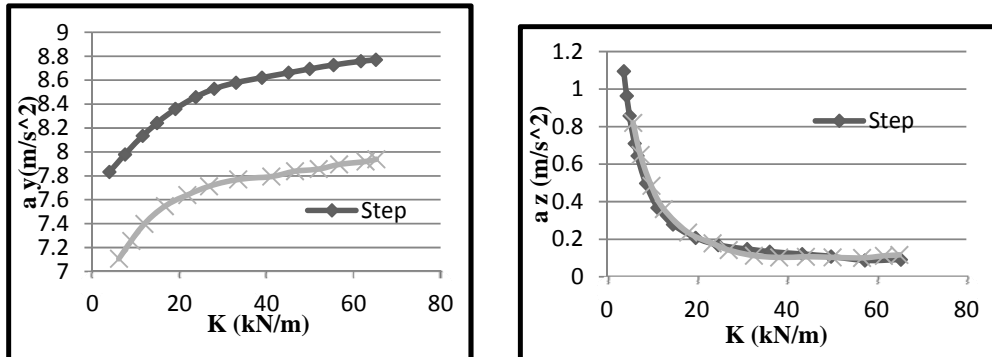


Fig. 11 The vehicle's maximum lateral and vertical acceleration

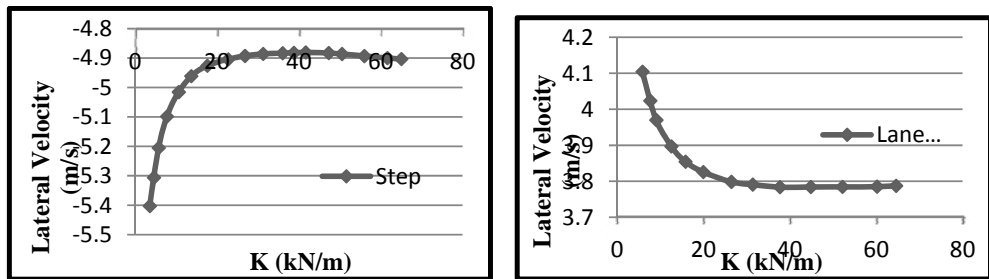


Fig. 12 The maximum value of lateral speed per step inputs and per Lane change

The third input in this study is when the right side of the vehicle passes through a bump as shown in Fig. 13 and the effects of the torsional stiffness are obtained on roll and yaw. The vehicle speed was assumed to be 54km/hr. As it can be seen in Fig. 14, increasing the stiffness parameters of the suspension system results in enhanced vehicle roll and yaw values. Fig. 15 shows the maximum lateral and vertical acceleration respectively, which they have been increased by increasing the torsional stiffness.

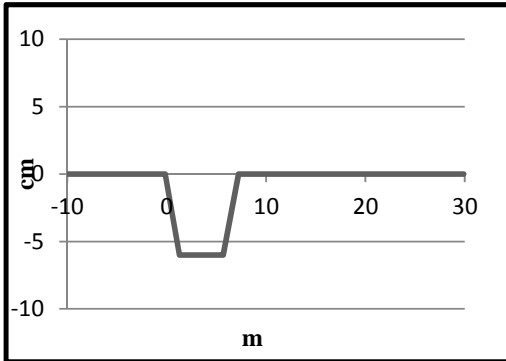


Fig. 13 Pit input.

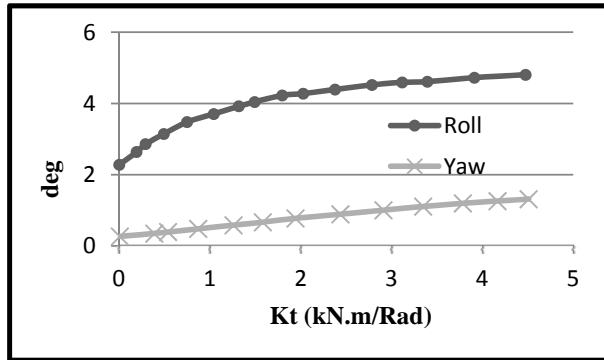


Fig. 14 the maximum body Roll and vehicle deviation based on changes in torsional stiffness for the pit input.

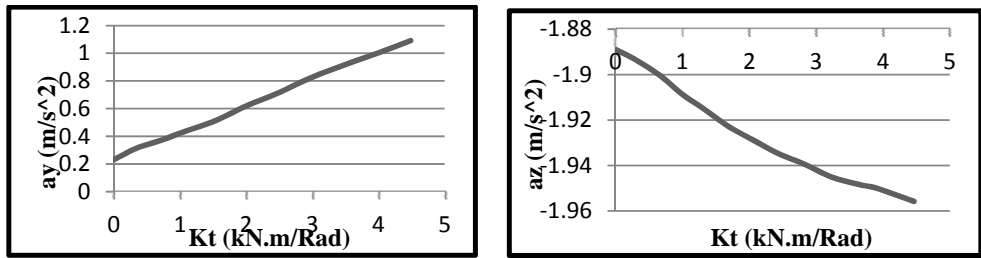


Fig. 15 the maximum lateral and vertical acceleration for the pit input.

## 6. Conclusions

The important quantity regarding ride comfort characteristics is the applied acceleration on the vehicle passengers. So the vehicle performance will be desired, when the lowest vertical acceleration is applied to the passengers. Therefore the diagrams of vertical acceleration were used to study the effect of stiffness and damping coefficient on ride comfort. In addition, the motions related to the handling and stability including transverse motion along y axis, yaw and roll motions was investigated. Regarding handling characteristics, the vehicle stability within a path means achieving a stable condition after an excitation. The vehicle performance is said to be desired if it has following conditions (a) The maximum angle of body roll has the minimum deviation from stable condition, (b) The maximum yaw angle has minimum deviation from stable condition (c) The above mentioned parameters reach to stable condition at less time and possible fastest period.

- 1 – The type of the applied input of the vehicle acts as an important factor in determining the effects of the vehicle stiffness and damping coefficients.
- 2 – The increase in vehicle stiffness and damping during the steering leads to decrease in pitch and roll values which this leads to enhanced stability.
- 3 - The increase in vehicle stiffness and damping while crossing the bump leads to increase in pitch and roll values.
- 4 – Whatever the value of the spring stiffness increases during turning, yaw is also increased which this facts results in reduction of turning radius.
- 6 - Maximum lateral and vertical acceleration of the vehicle increases with increasing torsional stiffness.

## R E F E R E N C E S

- [1]. *A. Afkar, M. Mahmoodi-kaleibar, A. Paykani*. Geometry optimization of double wishbone suspension system via genetic algorithm for handling improvement. *Journal of Vibroengineering*, Vol. 14 (2), pp. 827-837, 2012.
- [2]. *G.J. Heydinger*. Improved simulation and validation of road vehicle handling dynamics. Ph.D. Thesis, Ohio-state University, 1990.
- [3]. *S.K. Clark*, National bureau of standards monographs 122, 1971.
- [4]. *H. Pacejka*, Mechanics of pneumatic tires, USA, 1981.
- [5]. *H. Sakai*. Theoretical and experimental studies on the dynamic properties of tyres - 1. Review of theories of rubber friction. *International Journal of vehicle design*, Vol. 2, (1), pp. 78-110, 1981.
- [6]. *H. Sakai*. Theoretical and experimental studies on the dynamic properties of tyres part - 2. Experimental investigation of rubber friction and deformation of a tyre. *International Journal of vehicle design*, Vol. 2, (2), pp. 182-226, 1981.

- [7]. *H. Sakai*. Theoretical and experimental studies on the dynamic properties of tyres - 4. Investigations of the influences of running conditions by calculation and experiment. International Journal of vehicle design, Vol. 3, (3), pp. 333-375, 1982.
- [8]. *L. Segel*. Proceedings of the automobile division of the I.mech.E., **7**, 310, 1956.
- [9]. *W.C. Hamann*. SAE, paper number: 670192, 1967.
- [10]. *T. Maeda, H. Vemura*. SAE, paper number: 690233, 1969.
- [11]. *T. Kohno, S. Tsuchiya , N. Komoda*. SAE, paper number: 690488. 1969.
- [12]. *J.E. Ford, J.E. Thompson*. SAE, paper number: 690804, 1969.
- [13]. *Q. Zhu, M. Ishitobi*. Chaotic vibration of a nonlinear full-vehicle model . International Journal of Solids and Structures, **43**, 747, 2006.
- [14]. *S. Cation, J. Robert, O. Michele, P.D. James*. Six degree of freedom whole-body vibration during forestry skidder operations. International Journal of Industrial Ergonomics 38, 739 2008.
- [15]. *H.B. Pacejka, E. Bakker, L. Linder*, SAE, paper number: 890087 1989.
- [16]. *H.B. Pacejka, E. Bakker, L. Nybreg*. SAE, paper number: 8704211987.
- [17]. *A.G. Nelecz, A.C. Bindemann*. Analysis of the dynamic response of four wheel steering vehicles at high speed. International Journal of Vehicle design, 9 (2), 1988.
- [18]. *M. Demic*. Optimisation of the characteristics of the elasto-damping elements of a passenger car by means of a modified Nelder-Mean method. International Journal of Vehicle design, 10 (2), pp. 136-152, 1989.
- [19]. *X. Liu, J. Wagner*. Design of a vibration isolation actuator for automotive seating systems - Part I: Modelling and passive isolator performance. International Journal of Vehicle design, 29 (4), pp. 335-356, 2002.
- [20]. *X. Liu, J. Wagner*. Design of a vibration isolation actuator for automotive seating systems - Part II: Controller design and actuator performance. International Journal of Vehicle design, 29 (4), pp. 357-375, 2002.